Evolution of tidal disruption events from the XMM-Newton Slew Survey

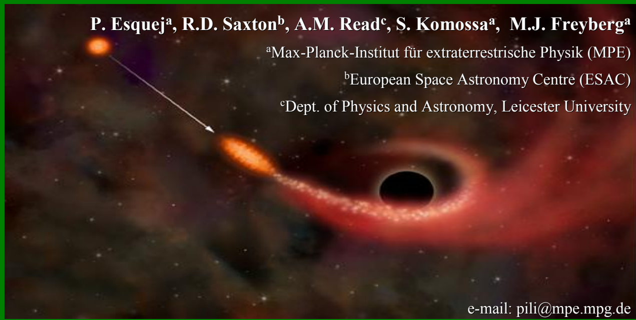

P. Esquej[a], R.D. Saxton[b], A.M. Read[c], S. Komossa[a], M.J. Freyberg[a]

[a]Max-Planck-Institut für extraterrestrische Physik (MPE)

[b]European Space Astronomy Centre (ESAC)

[c]Dept. of Physics and Astronomy, Leicester University

e-mail: pili@mpe.mpg.de

Dynamical studies assert that massive dark objects reside in the nuclei of many galaxy bulges. Dormant supermassive black holes can be unveiled by the detection of outburst radiation produced when a star is tidally disrupted and subsequently accreted by the nuclear black hole. A number of these exceptional events have been hitherto detected, being the two most recent ones discovered by XMM-Newton during slew observations.

Characteristics of tidal disruption events

- Stellar disruption when star approaches the black hole tidal radius.
- Non-recurrent flare is emitted with X-ray peak luminosity (Komossa et al. 2002):

$$L_{peak}(10^5 M_{sun} < M_{BH} < 10^8 M_{sun}) \sim \begin{cases} 10^{39} - 10^{42}\, erg\, s^{-1} \,(giant\ star) \\ 10^{43} - 10^{45}\, erg\, s^{-1} \,(main\ seq.\ star) \end{cases}$$

- Extreme X-ray softness in outburst: black body model with kT ~ 0.04 - 0.1 keV.
- Mass rate after one post-disruption orbit:

$$\dot{M} \approx \left(\frac{t - t_{disruption}}{1yr}\right)^{-5/3}$$ (Evans & Kochanek 1989; Ayal et al. 2000)

The XMM-Newton Slew Survey

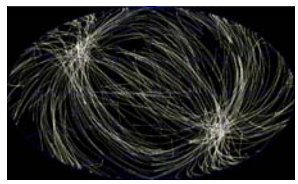

Fig. 1. Sky coverage of the slew survey in galactic coordinates.

- EPIC-pn in FF, eFF and LW mode.
- 10 seconds eff. on-axis exposure time.
- Low background.
- Positional accuracy: 8 arcsec (1σ).
- Flux limit:
  - Total band (0.2-12 keV): 1.2×10^{-12} erg/s/cm^2
  - Hard band (2-12 keV): 4×10^{-12} erg/s/cm^2
  - Soft band (0.2-2 keV): 6×10^{-13} erg/s/cm^2

(Saxton et al. 2008)

Candidates selection

Through comparison of the XMM-Newton Slew Survey and the ROSAT All-Sky Survey, two sources resulted in agreement with the tidal disruption model. They showed:

- soft X-ray spectra.
- high variability with respect to RASS 2σ-upper limits.

Table 1. Characteristics of the tidal disruption candidates.

Source(1,2)	Source type	Redshift	EPIC-pn/RASS upper limit	L_X(0.2-2.0keV)
NGC 3599	LLAGN	0.0028	88	3.9×10^{41} erg s^{-1}
SDSS J132341.97+482701.3	Normal galaxy	0.0875	83	1.4×10^{43} erg s^{-1}

(1) Optical spectra of the sources can be seen in Fig. 2, upper panels.
(2) Slew spectrum of NGC 3599 can be best fitted by a black body model with kT=95 eV. Fig. 2, lower panel.

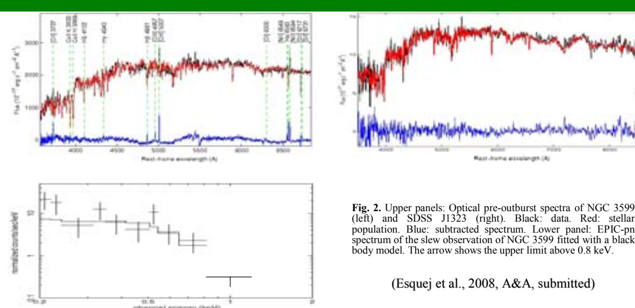

Fig. 2. Upper panels: Optical pre-outburst spectra of NGC 3599 (left) and SDSS J1323 (right). Black: data. Red: stellar population. Blue: subtracted spectrum. Lower panel: EPIC-pn spectrum of the slew observation of NGC 3599 fitted with a black body model. The arrow shows the upper limit above 0.8 keV.

(Esquej et al., 2008, A&A, submitted)

Follow-up observations: X-ray

- XMM-Newton

These are the nearest X-ray follow-up observations performed close to the outburst (roughly two years after the slew observations). NGC 3599 and SDSS J1323 have faded by factors of 27 and 40 respectively and have hardened with time. The best-fit model to the EPIC-pn spectra is a power-law model (Γ_X=3.0 and 3.4) with Galactic absorption (Fig.3).

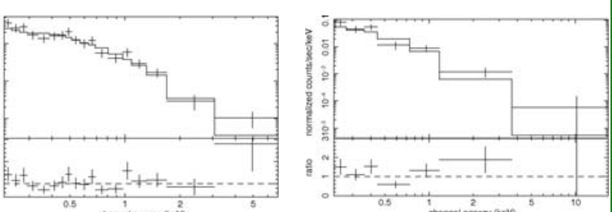

Fig. 3. EPIC-pn spectra of NGC 3599 (left) and SDSS J1323 (right) fitted by a power-law model plus Galactic absorption. Data/model residuals are presented at the bottom of each spectrum.

- Swift

Both sources were too weak at the time of the follow-up Swift observations to apply spectral fits but they were used to provide a further point in the light curve of the sources.

Follow-up observations: Optical

Optical post-outburst follow-up observations performed with the Nordic Optical Telescope and the Isaac Newton Telescope three years after the slew observations did not show any evident signature of the disruption event.

X-ray light curves of the flare events

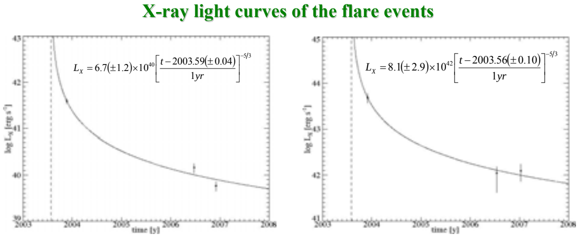

Fig. 4. X-ray light curves of the two tidal disruption events NGC 3599 (left) and SDSS J1323 (right). The points come from the XMM slew, XMM pointed and Swift observations from left to right in each plot. Solid lines are the fitted $t^{-5/3}$ curves presented in the corresponding equation in each panel. Dashed lines show the disruption time (t_{disr}) as returned by the fitting.

Table 2. Estimated lower limit properties of the disruption events.

Source	ΔE_X(1) (erg)	ΔM(2) (M_{sun})	R_X(3) (cm)
NGC 3599	7.1×10^{48}	4.0×10^{-5}	7.3×10^{11}
SDSS J132341.97+482701.3	7.6×10^{50}	4.2×10^{-3}	6.8×10^{12}

(1) Released energy during the outburst.
(2) Accreted mass in the total event.
(3) Radius of the emitting region.

Tidal disruption rate from the XMM-Newton Slew Survey

The identification of tidal disruption events here discussed was enabled by the existence of two large area sensitive X-ray surveys performed at different epochs.

The tidal disruption rate will be:

$$\frac{Number\ of\ events}{\int_0^{R_{max}} A(r)t(r)dr \times galaxy\ space\ density} \approx 2.3\times10^{-4}\, galaxy^{-1} yr^{-1}$$

where R_{max}=406 Mpc is our completeness distance, A(r) represents the covered area and t(r) is the flare duration depending on redshift (Fig. 5.)

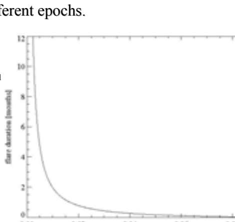

Fig. 5. Observable flare duration depending on redshift.

This result lies in fair agreement with theoretical predictions (Wang & Merrit 2004):

$$\dot{N} \approx 7.1\times10^{-4} yr^{-1}\left(\frac{\sigma}{70km\,s^{-1}}\right)^{7/2}\left(\frac{M_{BH}}{10^6 M_{sun}}\right)^{-1}\left(\frac{m_*}{M_{sun}}\right)^{-1/3}\left(\frac{R_*}{R_{sun}}\right)^{-1/4} \approx 7.0\times10^{-4} galaxy^{-1} yr^{-1}$$

considering a $10^6 M_{sun}$ black hole and a disrupted star of solar mass and radius.

References

Ayal, S., et al. 2000, ApJ, 545, 772
Esquej, P., et al. 2007, A&A, 462, L49
Evans, C. & Kochanek, C. 1989, ApJ, 346, L13
Komossa, S. 2002, Rev. in Mod. Ast, 15, 27
Saxton, R.D., et al. 2008, A&A, 480, 611
Wang, J. & Merrit, D. 2004, ApJ, 600, 149

The X-ray Universe 2008
27 - 30 May, Granada, Spain